Femtosecond CARS of Binary Liquid Mixtures: Dephasing via Concentration Fluctuations in the Intermediate Regime

F. Lindenberger, R. Stöckl, B. P. Asthana,† and A. Laubereau*

Physik-Department E11, Technische Universität München, D-85748 Garching, Germany

Received: April 14, 1999

The symmetric CH_3-stretching mode ν_1 of CH_3I is investigated in a solution of $CDCl_3$ in the concentration range 7−100% and temperature interval 242−374 K using time-resolved coherent anti-Stokes Raman scattering (CARS) with 250 fs pulses and magic polarization geometries. Striking deviations from simple exponential relaxation dynamics are reported for mixtures with mole fractions around 0.5. Analysis of the concentration dependence allows to distinguish the dephasing contribution of concentration fluctuations with correlation time >1 ps, indicating the intermediate case for this relaxation mechanism. The results are well described by the Knapp−Fischer model for concentration fluctuations, yielding a molecular residence time in the solvation layer of 1.1−3.2 ps in the temperature range 242−374 K in accordance with theoretical estimates.

1. Introduction

The rapid molecular motion in liquids at ambient temperatures in general leads to small deviations of the observed spectral band shape for a vibrational transition from a simple Lorentzian equivalent to exponential dephasing in time domain.[1] The corresponding values of the vibrational correlation time τ_c characterizing the time scale of the (dominant) relaxation mechanism[2] are well in the subpicosecond time domain, suggesting dephasing close to the homogeneous case in the neat liquid.[3] In liquid mixtures, the situation may be different, although previous investigations of spontaneous Raman spectroscopy could not unambiguously unravel the details of the relaxation dynamics.[4]

The time-resolved techniques have considerably advanced in recent years, introducing three-color fs-CARS.[5] A polarization technique was invented to separate the purely vibrational dynamics[6] and investigate dephasing mechanisms in several cases.[3,7] Echo techniques were developed and applied to a few number of systems, e.g. Raman echo measurements of molecular vibrations of several liquids.[8,9] For selected systems with particularly long dephasing times, infrared photon echo measurements could also be demonstrated.[10]

In this report, we demonstrate that the time domain CARS technique is well suited to study details of the relaxation process and observe deviations from the simple exponential case. The binary mixture CH_3I:$CDCl_3$ is investigated and shown to represent the intermediate relaxation case for concentrations around 50% with average correlation times τ_c up to 1 ps. Measurements of the concentration dependence allow to uniquely separate the dephasing contribution by concentration fluctuations, the time scale of which is determined to be 3.2−1.1 ps in the temperature range 242−374 K.

The system CH_3I:$CDCl_3$ was studied by IR spectroscopy more than two decades ago.[11,12] Döge et al.[4] carried out the first Raman study on the band shapes of ν_1 vibration of CH_3I in the neat liquid as well as in mixtures with $CDCl_3$. The line width of the ν_1 band displayed a peculiar concentration dependence with a maximum at a mole fraction of $x = 0.5$, in both the IR and Raman studies. Bondarev and Mardaeva[11] explained this dependence in terms of additional line broadening via slow concentration fluctuations assuming a stationary concentration distribution of Gaussian shape in a microscopic volume around the reference molecule. This assumption based on Anderson and Kubo theory[2,13] leads to a symmetric line-width dependence around $x = 0.5$ not observed for some examples. Knapp and Fischer[14,15] included the dynamical aspect into the theory, i.e., concentration fluctuations due to diffusion, in order to explain a more general type of concentration dependence and line broadening. The available spectroscopic data, however, did not allow to determine the time scale of the dephasing mechanism unambiguously. Muller et al.[8] reported recently evidence for spectral diffusion in Raman echo observations of the 50% mixture. From a comparison with CARS and conventional Raman data, an inhomogeneous broadening contribution was deduced with a lifetime of 4−7 ps at room temperature and assigned to concentration fluctuations.

2. Experimental Section

The basic features of the experimental setup were discussed in detail previously[6,7] and are only briefly described here. The main component is a pulsed, hybrid mode-locked dye laser, synchronously pumped by an amplified and frequency-doubled Nd:YLF laser[16] with repetition rate 50 Hz. After multipass dye amplification of a single pulse, part of the laser radiation is directed to a quartz plate for continuum generation. Out of the produced spectral broadening, two frequency bands are selected by pairs of interference filters and amplified in two additional dye amplifiers for the generation of Stokes-shifted and probing pulses with adjustable frequencies. Together with the second part of the laser pulse, three different input pulses of approximately 250 fs duration and 50−70 cm^{-1} width are accomplished for femtosecond CARS experiments. Using $\lambda/2$ plates and Glan polarizers, parallel polarization of the input laser and Stokes pulses is adjusted, while the polarization plane of the probe pulse is inclined by 60°. The coherent Raman scattering of the 2 mm sample cell is measured behind an analyzing polarizer in a small acceptance angle in phase-

* Corresponding author.
† On leave from Laser and Spectroscopy Laboratory, Department of Physics, Banaras Hindu University, Varanasi 221 005, India.

10.1021/jp991228f CCC: $18.00
Published on Web 06/26/1999

matching direction and at the proper anti-Stokes frequency position, using dielectric filters with a bandwidth of 80 cm^{-1}, adjustable neutral filters, and a photomultiplier. The mentioned polarization geometry allows to adjust magic angles θ for the orientation of the analyzer of the CARS signal.[6,7] The instrumental response function, determined by a measurement of the nonresonant scattering in carbon tetrachloride (see below, eq 3) decays exponentially over an accessible dynamic range of 10^6 with a slope of 1/60 fs^{-1}, the latter value indicating the available experimental time resolution.

3. "Magic" Three-Color CARS

The polarization interference in femtosecond CARS was demonstrated recently.[6] It was shown that the third-order nonlinear polarization responsible for coherent Raman scattering consists of three parts showing different time and polarization behavior:

$$P_{\mathrm{iso}}(t) = F_{\mathrm{iso}}E_{\mathrm{P}}(t-t_{\mathrm{D}}) \int_{-\infty}^{t} \phi_{\mathrm{vib}}(t\text{-}t')\, E_L(t')\, E_{\mathrm{S}}(t')^*\, \mathrm{d}t' \quad (1)$$

$$P_{\mathrm{aniso}}(t) = F_{\mathrm{aniso}}E_{\mathrm{P}}(t\text{-}t_{\mathrm{D}}) \int_{-\infty}^{t} \phi_{\mathrm{vib}}(t\text{-}t')\, \phi_{\mathrm{or}}(t\text{-}t')\, E_{\mathrm{L}}(t')\, E_{\mathrm{S}}(t')^*\, \mathrm{d}t' \quad (2)$$

$$P_{\mathrm{nr}}(t) = F_{\mathrm{nr}}E_{\mathrm{P}}(t\text{-}t_{\mathrm{D}})\, E_{\mathrm{L}}(t)\, E_{\mathrm{S}}(t)^* \quad (3)$$

The subscripts iso, aniso, and nr, respectively, label the isotropic, anisotropic, and nonresonant parts of the nonlinear polarization P that generates the CARS signal. E_{P}, E_{L}, and E_{S} denote the electric field amplitudes of the three input pulses (probe, laser, and Stokes) with corresponding frequency positions ω_{P}, ω_{L}, and ω_{S}. ϕ_{vib} and ϕ_{or}, respectively, represent the vibrational and orientational autocorrelation functions of individual molecules; a collective (delocalized) character of the vibrational modes is not included in the theoretical treatment that also assumes statistical independence of vibrational and reorientational relaxation. t_{D} is the delay time of the probe pulse relative to the coincident excitation pulses, laser and Stokes.

Equations 1 and 2 refer to the resonant case, $\omega_{\mathrm{L}} - \omega_{\mathrm{S}} = \omega_0$, where the latter quantity denotes the vibrational transition frequency. The polarization geometry enters into eqs 1−3 via the prefactors F that are explicitly known.[6] The F's are also governed by different coupling constants: the isotropic and anisotropic components of the Raman scattering tensor and the nonresonant part of the third-order nonlinear susceptibility enter alternatively eqs 1−3. The experimental CARS signal is proportional to the convolution integral of the intensity of the probing pulse $\propto E_{\mathrm{P}}(t\text{-}t_{\mathrm{D}})^2$ with the absolute value squared of the total third-order polarization, $|P|^2$. It was shown recently[6,7] that for three polarization situations (analyzer orientations θ) one of the three prefactors on the rhs of eqs 1−3 alternatively vanishes. The corresponding angles are the magic values $\theta =$ 49.1°, −30°, and −60°. The resulting CARS signal contains only the remaining two contributions and represents more specific information. Measurements with the three magic angles allow to determine the three scattering components with different time dependencies uniquely. It was also demonstrated that the proper deconvolution of the isotropic scattering component related to P_{iso} (see eq 1) from CARS data is crucial for a measurement of the correlation time τ_{c} of the vibrational relaxation process.[3]

4. Theoretical Models for Dephasing

As a consequence of linear response theory, the time evolution of a molecular vibration excited by two coherent optical fields, E_{L} and E_{S} (see eqs 1 and 2), is described by the vibrational autocorrelation function ϕ_{vib}, where

$$\phi_{\mathrm{vib}}(t) = \langle q(0)\, q(t) \rangle \quad (4)$$

Here the brackets $\langle\ \rangle$ represent an ensemble average over the molecules in the excitation volume and $q(t)$ is the quantum-mechanical expectation value of the vibrational amplitude generated by the pump fields. Neglecting pair correlation effects, the same expression governs the spectral bandshape in spontaneous Raman spectroscopy.[1] Using the Anderson−Kubo theory,[2,13] an explicit expression can be derived for this function ($t \geq 0$)[17]

$$\phi_{\mathrm{vib}}(t) = \exp\{-\tau_{\mathrm{c}}/T_2[\exp(-t/\tau_{\mathrm{c}}) - 1] - t/T_2\} \quad (5)$$

where two parameters, T_2 and τ_{c}, are introduced. The oscillatory part of ϕ_{vib} is omitted here. Equation 5 dwells on the assumption that the variations of the transition frequency of a molecule due to interaction with its environment follow a Gaussian distribution about a central frequency ω_0 with width $\Delta\omega$. The correlation time τ_{c} represents a (model-specific) measure of the time scale of the frequency fluctuations, the rms amplitude of which is given by Γ. The asymptotic exponential decay predicted by eq 5 is determined by the dephasing time T_2 and expected for very general arguments. T_2 is related to the other parameters by

$$T_2 = (\Gamma^2\tau_{\mathrm{c}})^{-1} \quad (6)$$

In the general case, more than one relaxation mechanism contributes notably to the dephasing of a vibrational transition. Assuming the relaxation processes to be statistically independent, the total autocorrelation function ϕ_{eff} results from a simple superposition of the individual mechanisms i with autocorrelation functions $\phi_{\mathrm{vib},i}$ according to

$$\phi_{\mathrm{eff}}(t) = \prod_{i}^{m} \phi_{\mathrm{vib},i}(t) \quad (7)$$

where m is the number of relaxation channels. The $\phi_{\mathrm{vib},i}$ are governed by their individual parameter sets $T_{2,i}$, $\tau_{\mathrm{c},i}$, and Γ_i. The asymptotic relaxation behavior predicted by eqs 5 and 7 is again exponential with effective dephasing rate $1/T_2 = \sum 1/T_{2,i}$, i.e., additive individual rates.

In the following we will confine ourselves to the explicit discussion of two relaxation processes, only, for a molecule A (in the following, CH_3I) in the binary mixture with solvent B (e.g. $CDCl_3$), yielding $\phi_{\mathrm{eff}} = \phi_{\mathrm{a}}\phi_{\mathrm{b}}$ from eq 7; the subscript vib is omitted in the following. The first relaxation channel (a) represents the effect of concentration fluctuations of neighboring molecules A and B in the solvation layer around the probed molecule and will be discussed below in more detail. The second mechanism (b) accounts for the dephasing in the neat liquid A that may originate from the repulsive part of the intermolecular interaction including energy relaxation.[18] A third mechanism (c), accounting for the corresponding dephasing interaction of the sample molecule A with solvent molecules B, will be assumed to numerically equal to mechanism (b) within experimental accuracy and thus incorporated in ϕ_{b}.

Knapp and Fischer[14,15] developed a theoretical model for the vibrational dephasing of binary liquid mixtures that is analytically tractable due to certain model assumptions. According to this approach, the probed molecule A in a mixture A + B is influenced by a certain number N of nearest neighbors ($N \leq$ 8). The nearest neighbor can be a type A or a type B molecule,

depending on concentration, and influences the probed molecule independently and irrespective of whether another neighbor is of type A or B. Now, the vibrational frequency and line width of A is found in general to be concentration dependent; as a consequence, the exchange of a type A by a type B molecule in the solvation layer is assumed to cause a frequency shift $\Delta\omega$ and a change in bandwidth $\Delta\gamma$. Interaction with non-nearest neighbors is neglected. With respect to the experimental situation, we restrict the following discussion of the theoretical model to the special case $\Delta\gamma = 0$. The vibrational frequency of reference molecule A is given by

$$\omega = \omega_0 - (N/2 - n_B)\Delta\omega \tag{8}$$

where n_B is the momentary number of molecules B in the solvation layer ($0 \le n_B \le N$). Equation 8 leads to a binomial frequency distribution ω replacing the Gaussian distribution mentioned above in context with eq 5. n_B varies in the liquid because of diffusion. For rapid changes in the solvation shell, the frequency jumps $\Delta\omega$ are smeared out and motional narrowing occurs similar to the Anderson−Kubo theory. Introducing a constant exchange rate R for the molecules in the solvation shell (same value for molecules A and B) and assuming that the replacement of a molecule in the shell does not involve a phase change of the vibrating sample molecule A, the Knapp−Fischer model arrives at the autocorrelation function ($t \ge 0$):

$$\phi_1(t) = \{\exp(-st)[\cosh(rt) + s/r \sinh(rt)]\}^N \tag{9}$$

Here the complex quantities s, r are introduced that depend on concentration; for our special case $\Delta\gamma = 0$, they read

$$s = R/2 - i(x - {}^1/_2)\Delta\omega \tag{10}$$

and

$$r = \{[(R^2 - \Delta\omega^2)^2 + 4(2x-1)^2\Delta\omega^2R^2]^{1/2} + R^2 - \Delta\omega^2\}^{1/2}/2^{3/2} - i\Delta\omega\{[(R^2 - \Delta\omega^2)^2 + 4(2x-1)^2\Delta\omega^2R^2]^{1/2} - R^2 + \Delta\omega^2\}^{1/2}/|2^{3/2}\Delta\omega| \tag{11}$$

The concentration, i.e., mole fraction of A is denoted by x. In the following the model is used for comparison with experimental data only in the case $R > |\Delta\omega|$, where its discrete frequency distribution is smeared out by motional narrowing. Equation 9 supplemented by eqs 10 and 11, may be considered as a special formulation of ϕ_a mentioned above, with an explicit prediction of the concentration dependence. For short t, ϕ_1 decays nonexponentially in qualitative agreement with eq 5. For large t, ϕ_1 recovers the expected exponential decay representing the Markovian limit with decay rate

$$1/T_{2,a} = NR/2 - N\{[(R^2 - \Delta\omega^2)^2 + 4(2x-1)^2\Delta\omega^2R^2]^{1/2} + R^2 - \Delta\omega^2\}^{1/2}/2^{3/2}\} \tag{12}$$

In the limit of very fast motional narrowing, $R \gg \Delta\omega$, eqs 9−11 predict simple exponential decay, as required for dephasing in the homogeneous limit, with $1/T_{2,a} = \Delta\omega^2[1 + (2x-1)^2]N/(4R)$.

The additional relaxation mechanisms (b) and (c) besides concentration fluctuations in the solvation shell, mentioned above, are expressed in the model by simple exponentials, i.e., assuming $\tau_{c,i} \simeq 0$ for the corresponding processes ($i = 2, 3$; see eq 5). The corresponding dephasing rates can be condensed into a single constant $1/T_{2,b}$, so that we simply have ($t \ge 0$):

$$\phi_2(t) = \exp(-t/T_{2,b}) \tag{13}$$

Rewriting eqs 7, we arrive at the total autocorrelation function ($t \ge 0$):

$$\phi_{KF}(t) = \phi_1(t)\,\phi_2(t) \tag{14}$$

The Knapp−Fischer theory contains only two important parameters, R and N, while the other phenomenological quantities are readily determined from spontaneous Raman spectroscopy and/or CARS measurements. ω_0 and $\Delta\omega$ are obtained from the frequency position of the Raman line in the neat liquid and the line shift $\Delta\Omega$ upon infinite dilution, $\Delta\omega = \Delta\Omega/N$. Measurements of the dephasing rate $1/T_2(x=1)$ and $1/T_2(x\to0)$ or corresponding Raman line widths deliver the value of $T_{2,b} = T_2(x=1)$ and also allow to verify the special case $\Delta\gamma = [1/T_2(x\to0) - 1/T_2(x=1)]/N \simeq 0$ as assumed for the present discussion. The validity of the approximations τ_{c2}, $\tau_{c3} \simeq 0$ entering eq 13 may be also checked by an analysis of data for the two concentration limits.

5. Time-Resolved Measurements Using Three-Color CARS

We have investigated the symmetric CH_3-stretching mode ν_1 of CH_3I in the neat liquid and 11 different mixtures with deuterated chloroform with mole fractions of the reference molecule in the range $x = 0.076-0.958$. The system was investigated previously by spontaneous Raman spectroscopy, but the details of the relaxation processes, e.g. the dynamics of the concentration fluctuations, could not be clearly determined.[4,15] The ν_1 frequency is $\omega_0/2\pi c = 2950$ cm^{-1} in the neat liquid and varies approximately linearly with dilution. The line width (isotropic scattering component) in the neat liquid is 4.8 cm^{-1} with approximately the same value for infinite dilution, suggesting $\Delta\gamma \simeq 0$. For the 1:1 mixture ($x = 0.5$), the considerably larger line width of $\simeq$8.6 cm^{-1} suggests a pronounced effect of concentration fluctuations.[4] Some examples of our time-resolved CARS data are presented in Figure 1a−c for 298 K and concentrations of $x = 0.076$, 0.47, and 0.916, respectively. The data refer to the magic angle $\theta = 49.1°$ suppressing, the anisotropic scattering contribution that would perturb the determination of the τ_c's. As a consequence, only the isotropic scattering component providing the information on the vibrational dynamics (see eq 1) and the nonresonant part contribute to the signal transients. The latter produces the signal overshoot around zero delay and rises with increasing solvent concentration ($1 - x$). The nonresonant scattering allows to check the instrumental response function (dotted lines) and provides in situ information on the zero-delay setting that is important for a proper determination of τ_c. For larger delay, $t_D > 2$ ps, the signal curve approaches an exponential decay with slope $2/T_2$ and finally reaches a constant background amplitude, indicating the limit of detectability of the coherent scattering. It is interesting to see the pronounced deviation from the exponential slope in Figure 1b for short delay time, $0.5 < t_D < 2$ ps ($x = 0.47$), indicating a rather large correlation time around 1 ps, or correspondingly, a relatively small exchange rate R. The logarithmic ordinate scales in Figure 1a−c should be noted. In the same experimental runs we have also measured the signal transients for the other magic angles, $\theta = -30°$ and $-60°$, providing supplementary information on the dephasing dynamics (data not shown).

In another set of measurements, the binary mixture CH_3I:$CDCl_3$ was studied at fixed concentration $x = 0.515$ as a

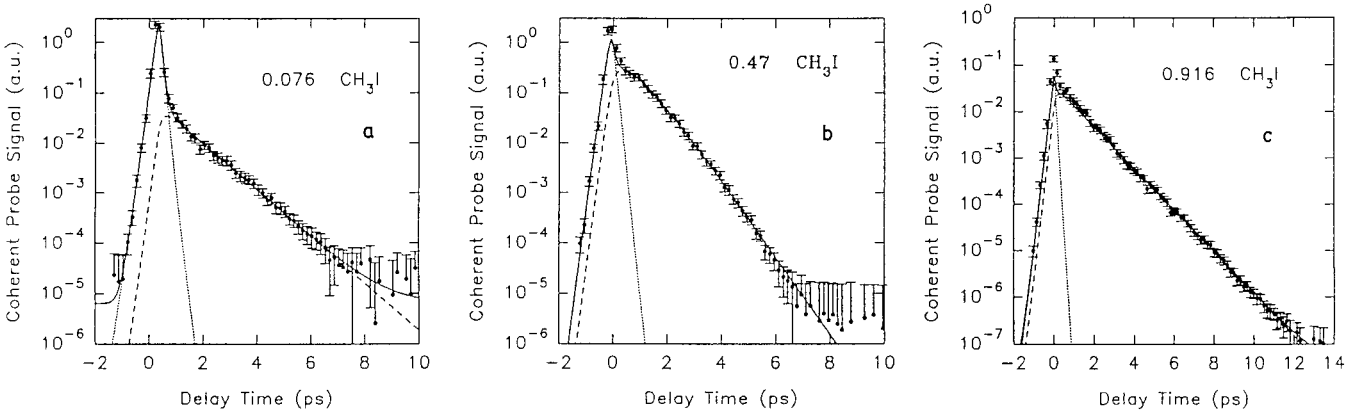

Figure 1. Coherent probe scattering signal of the symmetric stretching vibration ν_1 of CH_3I in the mixture with $CDCl_3$ vs delay time for the magic angle $\theta = 49.1°$ and three mole fractions of CH_3I: $x = 0.076$ (a), 0.47 (b), and 0.916 (c); experimental points (298 K); calculated curves: isotropic scattering component (dashed), nonresonant part (dotted), and total CARS signal (solid line).

function of temperature in the range 242−374 K. Since the mixture has a boiling point of ≃325 K at ambient pressure, a minor pressure increase up to 5×10^5 Pa of the sample was used. The small increase of several bars is expected to have a negligible effect on the dephasing dynamics only.[19] The CARS signals for two temperature values, 271 and 374 K, are presented in Figure 2 ($\theta = 49.1°$). The different curvatures and asymptotic slopes of the signal curves directly indicate significant changes of the dephasing mechanism.

6. Data Analysis and Discussion

The experimental results are interpreted using three different models:

(i) A single Rothschild function, eq 5, is fitted to the signal transients, yielding an average correlation time τ_c and an effective dephasing time T_2 of the involved dephasing processes in the various mixtures.

(ii) An effective autocorrelation function consisting out of two Rothschild functions, $\phi_{eff} = \phi_a\phi_b$, is used for the data analysis (eqs 5 and 7). The first factor ϕ_a represents the effect of concentration fluctuations with parameter values $\tau_{c,a}$ and $T_{2,a}$ depending on concentration. In the limiting cases $x = 0$, 1, the mechanism (a) disappears and only the second factor ϕ_b, again of the form of eq 5, remains. The latter combines the effect of energy relaxation and additional pure dephasing processes, e.g. via the repulsive part of the intermolecular interaction. Because of the equal values of the dephasing time (and line width) measured for $x = 1$ and $x \rightarrow 0$, $T_{2,b}$ is taken to be concentration independent. With respect to the large experimental error of short correlation times, we make the simplifying assumption that also $\tau_{c,b}$ is concentration independent and given by the value measured for the neat liquid CH_3I (150 ± 150 fs).

(iii) The time-resolved scattering data are analyzed in terms of the Knapp−Fischer model with the functions ϕ_1 and ϕ_2 making up the total autocorrelation function (eqs 9, 13, 14). For the simple case $\Delta\gamma \simeq 0$, ϕ_2 is concentration independent. Comparing with case (ii), we note that ϕ_2 corresponds to ϕ_b with the simplification $\tau_{c,2} \rightarrow 0$; the latter assumption is numerically insignificant in the following for the determination of a molecular residence time $1/R$ of a few picoseconds in the solvation layer.

The effect of resonant intermolecular coupling will be neglected in our data analysis of the symmetric stretching mode ν_1. Oehme et al. carried out a detailed study of such effects for CH_3I and its isotopic derivatives in various solvents.[20] For the ν_1 mode, only small effects were reported. Isotopic dilution of methyl iodide, for example, does not change the ν_1 linewidth

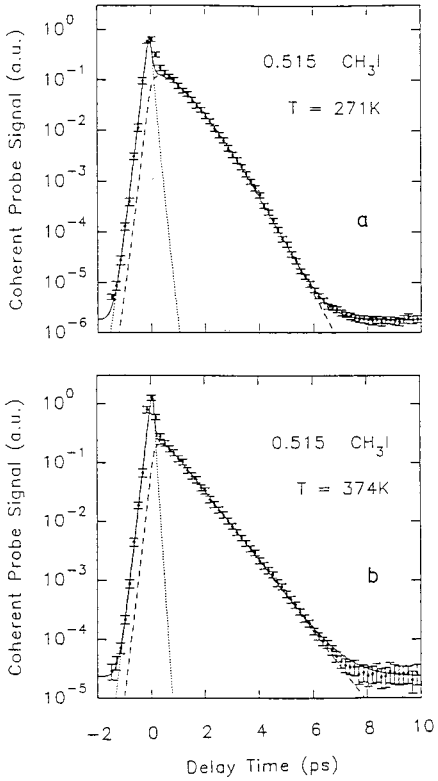

Figure 2. Same as Figure 1, but for $x = 0.515$ and two temperature values: 271 K (a) and 374 K (b).

within the measuring accuracy of approximately 2%, while the line is slightly blue-shifted by ≃1.5 cm^{-1} in the low-concentration limit.[21]

(a) Concentration Dependence. The solid curves in Figures 1 and 2 represent the computed results of the fitting procedure for case (i) to reproduce the experimental points. For the two other situations the agreement between calculated and measured data is even better. The results for the dephasing parameters of the approaches (i) and (ii) are presented in Table 1. The effective dephasing times T_2 and average correlation time τ_c referring to analysis (i) are listed in columns 2 and 3. The same data are depicted also in Figure 3. It is interesting to notice the shortening of the dephasing time with decreasing concentration from the neat liquid, $x = 1$, to $x \simeq 0.5$ by a factor of ≃2 and the subsequent rise again with further dilution. The average correlation time simultaneously increases from a value around 0.1 to ≃1 ps and drops again. The changes indicate a strong contribution

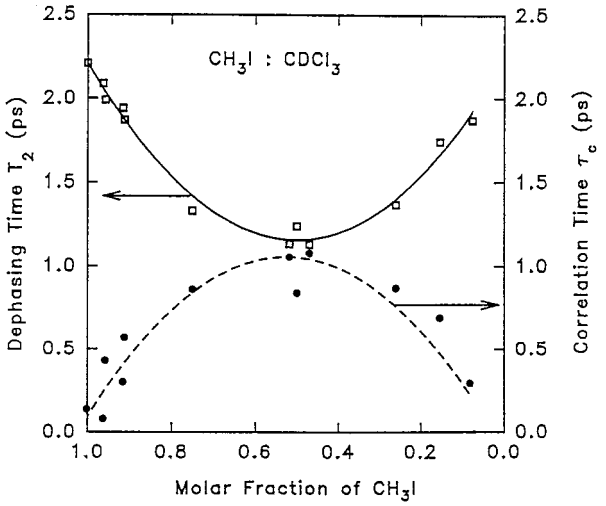

Figure 3. Measured effective dephasing time T_2 (open squares) and average correlation time τ_c (full points) of the ν_1 mode of CH_3I vs molar fraction x of CH_3I in the mixture with $CDCl_3$ (298 K); a single Rothschild function was fitted to the experimental data; curves are drawn as guides for the eye.

TABLE 1: Concentration Dependence of Dephasing Parameters of CH_3I:$CDCl_3$ at 298 K Derived from Three-Color Femtosecond CARS and Three Theoretical Models (Molar Fraction x)

x	T_2 (ps)	τ_c (ps)	$T_{2,a}$ (ps)	$\tau_{c,a}$ (ps)	$1/R$ (ps)
1.000	2.28 ± 0.02	0.15 ± 0.15			
0.958	1.99 ± 0.05	0.43 ± 0.2	16 ± 3	1.3 ± 0.8	2.0 ± 0.7
0.916	1.94 ± 0.05	0.3 ± 0.2	13 ± 2	0.8 ± 0.7	1.1 ± 0.7
0.912	1.87 ± 0.05	0.57 ± 0.2	10 ± 2	1.6 ± 0.8	2.1 ± 0.7
0.750	1.33 ± 0.05	0.86 ± 0.2	3.2 ± 0.3	1.5 ± 0.5	2.1 ± 0.4
0.515	1.14 ± 0.10	1.06 ± 0.4	2.3 ± 0.4	1.8 ± 0.7	2.0 ± 0.3
0.500	1.24 ± 0.10	0.84 ± 0.3	2.7 ± 0.5	1.4 ± 0.4	1.8 ± 0.3
0.470	1.13 ± 0.05	1.08 ± 0.2	2.2 ± 0.2	1.8 ± 0.4	2.2 ± 0.7
0.260	1.37 ± 0.10	0.87 ± 0.3	3.4 ± 0.6	1.6 ± 0.7	1.6 ± 0.5
0.154	1.74 ± 0.10	0.69 ± 0.4	7.3 ± 2	1.7 ± 1	1.4 ± 0.5
0.076	1.87 ± 0.10	0.3 ± 0.3	10 ± 3	<2	2.0 ± 0.4

of concentration fluctuations to the phase relaxation with a remarkably slow time scale of the process. More detailed insight is provided by a deconvolution of the latter process using approach (ii) for the data analysis. The corresponding results on $T_{2,a}$ and $\tau_{c,a}$ are compiled in columns 4 and 5 of Table 1. For the former constant, one simply has $1/T_{2,a} = 1/T_2 - 1/T_{2,b}$, with $T_{2,b} = 2.28 \pm 0.02$ ps (see T_2 value for $x = 1$); the T_2 values are displayed in column 1. The maximum efficiency of the concentration fluctuations is indicated by the minimum values of $T_{2,a} \simeq 2.3$ ps around $x = 0.5$. For the correlation time, on the other hand, the data suggest an approximately constant value, independent of concentration. An average number of $\tau_{c,a} = 1.4 \pm 0.4$ ps is deduced from the data. The result corresponds to relaxation in the intermediate case for the 1:1 mixture as indicated by the ratio $\tau_{c,a}/T_{2,a} \simeq 0.6$. Several picoseconds are required to establish the asymptotic decay rate, i.e., reach the Markovian limit. For mixtures with notably larger and smaller concentrations, the mechanism approaches the homogeneous limit.

We have also analyzed the signal transients using the Knapp−Fischer model (iii). Since the value of $\Delta\Omega = 1.98 \pm 0.04$ ps^{-1} is known from Raman spectroscopy,[4] only two parameters are left open, the exchange rate R and the number of the nearest neighbors N. Now, by the help of eq 14 the product NR is already uniquely fixed by $\Delta\Omega$ and the dephasing rate $1/T_{2,a}$ at concentrations around $x = 0.5$, yielding $RN = 2.7 \pm 0.15$ ps^{-1}. In fact, the resulting concentration dependence of $T_{2,a}$ (column 4 of Table 1) is fully consistent with the prediction of eq 12

TABLE 2: Dephasing Data of the ν_1 Mode of CH_3I in the Mixture with $CDCl_3$ ($x = 0.515$) for the Temperature Range 242−374 K

temp (K)	T_2 (ps)	τ_c (ps)	$T_{2,a}$ (ps)	$1/R$ (ps)
242	0.85 ± 0.05	1.8 ± 0.4	1.4 ± 0.15	3.2 ± 0.2
265	0.94 ± 0.05	1.3 ± 0.4	1.6 ± 0.15	3.0 ± 0.4
271	0.98 ± 0.05	1.2 ± 0.4	1.7 ± 0.15	3.0 ± 0.3
298	1.14 ± 0.10	1.1 ± 0.4	2.3 ± 0.4	2.0 ± 0.3
321	1.10 ± 0.10	1.2 ± 0.4	2.1 ± 0.4	1.6 ± 0.2
374	1.48 ± 0.05	0.4 ± 0.2	4.2 ± 0.5	1.1 ± 0.2

(data not shown). It is important to note that the factors R and N can be separately determined from the nonexponential part of the signal transients fitting eqs 1 and 14 and supplementary expressions to the data. The model fully accounts for the pronounced curvature of the signal curves, i.e., delayed onset of the asymptotic decay rate for a sufficiently small value of R. Results are shown in the last column of Table 1. For easy comparison with $\tau_{c,a}$ the residence time $1/R$ of molecules in the solvation layer is listed. Within experimental accuracy, our measurements support the constant value of R as anticipated for the model; the average value amounts to $R = 0.55 \pm 0.1$ ps. The corresponding number of neighbors in the solvation layer is $N = 5.0 \pm 0.9$. This is a reasonable value, since not all nearest neighbors can efficiently interact with the CH_3-vibration because of the large size of the iodine atom.

The Anderson−Kubo model (ii) and the Knapp−Fischer theory (iii) both account for the observed dephasing via concentration fluctuations. The numerical difference between $\tau_{c,a}$ and $1/R$ (average values 1.4 ps versus 1.8 ps) reflects the varying model assumptions, i.e., the Gaussian versus binomial distribution for the frequency fluctuations of the vibration. It is felt, however, that the Knapp−Fischer model provides more detailed insight into the dephasing via concentration fluctuations because of explicit predictions on the signal transient as a function of concentration and the parameters R, N, and $\Delta\Omega$.

(b) Temperature Dependence. The temperature dependence of the dephasing processes allows an additional test of the Knapp−Fischer model. A liquid mixture with $x = 0.515$ is investigated where the effect of the concentration fluctuations is close to its maximum. For comparison, also the neat liquid CH_3I was studied, where no temperature dependence of T_2 was found within experimental accuracy. The considerably different behavior of the mixture is directly visible from the signal transients of Figure 2. Analysis of the data in terms of the approaches (i) and (iii) yields the results compiled in Table 2. Columns 2 and 3 display the effective dephasing time T_2 and average autocorrelation time τ_c related to model (i). The numbers reveal a considerable temperature variation of the concentration fluctuations that is also illustrated by Figure 4. τ_c displays a shortening with rising temperature by a factor of approximately 4 in the range 240−380 K that is qualitatively reasonable because of the faster thermal motion. The opposite effect for the effective dephasing time may be explained by motional narrowing. Analysis of the scattering data in terms of the Knapp−Fischer model (iii) confirms the result $N \simeq 5$ obtained above. The results for the inverse exchange rate $1/R$ are listed in the last column of Table 2. A decrease from 3.2 ps (at 242 K) to 1.1 ps (374 K) is found. The exchange rate is plotted in Figure 5 as a function of temperature (experimental points).

It is interesting to compare the experimental numbers with estimates of R from jump diffusion.[18,22] Using viscosity data available in the temperature range 0−40 °C,[23] the exchange rate was estimated and plotted in the figure (solid curve). The agreement of the predicted temperature change with the experimental numbers is noteworthy. The data provide further

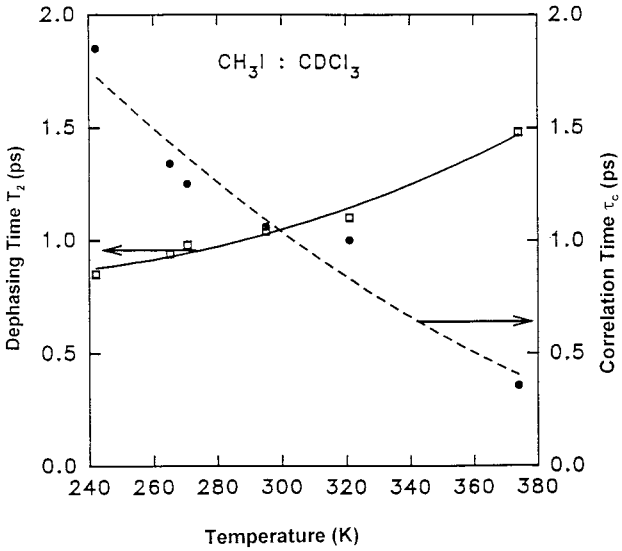

Figure 4. Measured effective dephasing time T_2 (open squares) and average correlation time τ_c (full points) for the ν_1 mode of CH_3I vs temperature in the mixture with $CDCl_3$ for constant concentration $x = 0.515$. The lines are drawn as a guide for the eye.

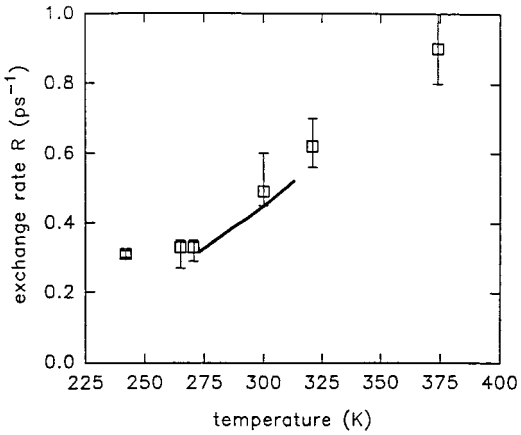

Figure 5. Measured exchange rate R (experimental points) as a function of temperature for the solvation layer containing $N \simeq 5$ molecules that contribute to the dephasing of the probing molecule CH_3I; the data are derived from the mixture with molar fraction $x = 0.515$ using the Knapp−Fischer model. The solid line is estimated for jump diffusion from available viscosity data. Rapid concentration fluctuations are found leading to dephasing in the intermediate regime.

evidence that concentration fluctuations are responsible for the observed dephasing channel.

Recently, Muller et al.[8] reported Raman echo and time-resolved two-color CARS measurements of the ν_1 mode of CH_3I in the 1:1 mixture with $CDCl_3$ (mole fraction 0.5) that were discussed in terms of dephasing via concentration fluctuations. An inhomogeneous broadening contribution of $\simeq 5$ cm^{-1} was inferred from the data with a lifetime of the inhomogeneity of 4−7 ps (spectral diffusion time, correlation time; data refer presumably to room temperature). The analysis of the Raman echo measurements corresponds to our model (ii) neglecting the finite correlation time for the concentration-independent part, $\tau_{c,b} \simeq 0$ (the latter approximation is numerically insignificant). The analysis of the time-resolved CARS data of ref 8, on the other hand, with deconvolution of the signal decay into a Gaussian and exponential part anticipates a long correlation time of the first dephasing mechanism. Our results are qualitatively similar but quantitatively different, e.g. $\tau_{c,a} \simeq 1.6 \pm 0.5$ ps at 298 K. The origin of the differences is not clear at the present time. We note that in our work with notably shorter pulses the nonresonant scattering contribution is suppressed by magic polarization conditions and need not be deconvolved from the signal transients as is the case for general polarization conditions. It may be expected that a nonresonant signal contribution may also occur in the Raman echo technique for temporal overlap of the two excitation pulse pairs. Our data are supported by the measured temperature dependence of the dephasing phenomena. The present analysis of three-color fs-CARS with magic polarization suggests that the frequency changes via concentration fluctuations develop on a time scale comparable to the dephasing time of the vibrational transition so that the mechanism is not close to the inhomogeneous broadening limit but in the intermediate modulation regime.

7. Conclusions

In summary, we wish to emphasize the potential of time-resolved three-color CARS for detailed information on molecular processes. We have demonstrated that the dynamics of concentration fluctuations can be derived from time-resolved dephasing observations using the Knapp−Fischer theory. Obviously, the dephasing rate and the time scale of the mechanism can be more precisely measured in time domain at the present time as compared to line-width and line-shape data in frequency domain; the latter did not allow to determine the exchange rate. Some of the simplifying assumptions of the theoretical model were confirmed by the present investigation; with some improvements providing better measuring accuracy, further details may become experimentally accessible so that modifications of the theory will be required in the future, e.g., different residence times of species A and B and/or a finite time interval to exchange a molecule in the solvation layer. Dephasing of a coherently excited vibrational transition has not yet been fully exploited for the investigation of intermolecular interaction in condensed matter.

References and Notes

(1) Laubereau, A.; Kaiser, W. *Rev. Mod. Phys.* **1978**, *50*, 607.
(2) Kubo, R. In *Fluctuation, Relaxation and Resonance in Magnetic Systems*; Ter Haar, D., Ed.; Plenum: New York, 1962; p 23.
(3) Lindenberger, F.; Rauscher, C.; Purucker, H.-G.; Laubereau, A. *J. Raman Spectrosc.* **1995**, *26*, 835.
(4) Döge, G.; Arndt, R.; Bühl, H.; Betterman, G. *Z. Naturforsch. A* **1980**, *35*, 468.
(5) Fickenscher, M.; Laubereau, A. *J. Raman Spectrosc.* **1990**, *21*, 857. Fickenscher, M.; Purucker, H.-G.; Laubereau, A. *Chem. Phys. Lett.* **1992**, *191*, 182.
(6) Li, W.; Purucker, H.-G.; Laubereau, A. *Opt. Commun.* **1992**, *94*, 300.
(7) Purucker, H.-G.; Tunkin, V.; Laubereau, A. *J. Raman Spectrosc.* **1993**, *24*, 453.
(8) Muller, L. J.; Bout, D. V.; Berg, M. *J. Chem. Phys.* **1993**, *99*, 810.
(9) Inaba, R.; Tominaga, K.; Tasumi, M.; Nelson, K. A.; Yoshihara, K. *Chem. Phys. Lett.* **1993**, *211*, 183.
(10) Tokmakoff, A.; Kwok, A. S.; Urdahl, R. S.; Francis, R. S.; Fayer, M. D. *Chem. Phys. Lett.* **1995**, *234*, 289.
(11) Bondarev, A. F.; Mardaeva, A. I. *Opt. Spectrosc.* **1973**, *35*, 167.
(12) Fujiyama, T.; Kakimoto, M.; Suzuki, T. *Bull. Chem. Soc. Jpn.* **1976**, *49*, 6.
(13) Anderson, P. W. *J. Phys. Soc. Jpn.* **1954**, *9*, 888.
(14) Knapp, E. W.; Fischer, S. F. *J. Chem. Phys.* **1981**, *74*, 89.
(15) Knapp, E. W.; Fischer, S. F. *J. Chem. Phys.* **1982**, *76*, 4730.
(16) Lindenberger, F.; Stöckl, R.; Laenen, R.; Laubereau, A. *Opt. Commun.* **1995**, *117*, 268.
(17) Rothschild, W. G. *Dynamics of Molecular Liquids*; Wiley: New York, 1983.
(18) Fischer, S. F.; Laubereau, A. *Chem. Phys. Lett.* **1975**, *35*, 6.
(19) Aechtner, P.; Laubereau, A. *Chem. Phys.* **1991**, *419*, 419.
(20) Keutel, D.; Seifert, F.; Oehme, K.-L. *J. Chem. Phys.* **1993**, *99*, 7463.
(21) Keutel, D. Thesis, Friedrich-Schiller-Universität Jena, 1993.
(22) Egelstaff, P. A. *An Introduction to the Liquid State*; Clarendon: Oxford, UK, 1992.
(23) *Beilsteins Handbuch der Organischen Chemie*, 4th ed.; Springer: Berlin, 1972; Vol. 1, part 1.